Journal of Manufacturing Engineering, 2007, Vol.2, Issue.2

DEVELOPMENT OF INTERNAL STRESSES IN NI-BASE SUPERALLOY DURING CYCLIC LOADING

S. Chaudhuri[1*], W. Chen[2] and R. P. Wahi[3]

[1]National Metallurgical Laboratory, Jamshedpur, India.
[2]Hahn-Meitner-Institute, Berlin, Germany.
[3]Retired from Hahn -Meitner-Institute, Berlin, Germany.

***E-mail :** sc1@nmlindia.org

ABSTRACT

Ni-base superalloy are extensively used as gas turbines and aero engine components because of their high temperature deformation resistance. In single crystal form Ni-base Superalloy SC16, consisting of 40% γ precipitates in the matrix of γ phase finds application in aero engines due to their improved high temperature resistance as compared to conventionally cast polycrystalline alloys. Deformation behaviour of this alloy under cyclic loading is interrelated in a complex manner with the state of internal stresses, material parameters such as volume fraction of γ precipitates, single crystal orientation, dislocation network at γ/γ′ interfaces as well as testing parameters such as temperature, strain rate, strain range etc. Keeping this in view, the state of internal stresses, characterized as back stress and friction stress developed during Low Cycle Fatigue (LCF) loading have been quantitatively estimated for the first time from the analysis of large volume of σ-ε hysteresis loops generated experimentally in the temperature range of 750ºC to 950ºC and total strain range of 0.8% to 2.0%, the strain rate of 10^{-3}/s remaining constant. Analysis of σ - ε hysteresis loops generated during LCF loading revealed that both back stress and friction stress, as a function of number of load cycles, attains almost a steady state at a constant temperature and strain range after an initial short transition region. The steady state value of back stress increases with increasing total strain range and decreasing temperature. In contrast, the steady state friction stress almost remains unaltered with these parameters.

Keywords: LCF,

1. INTRODUCTION

Nickel-base superalloys are widely used as gas turbine components. In single crystal form, they find application in aero engines due to their improved high temperature resistance as compared to conventionally cast polycrystalline alloys. A recently developed single crystal superalloys for blade application in land base gas turbines is SC16. The high temperature strength in this alloy is mainly due to dispersion of ordered ($L1_2$) inter-metallic compound (γ) in the matrix of nickel solid solution (γ). The alloy contains approximately 40% γ precipitates [1,2]. The mechanical behavior of this alloy under monotonic loading has been extensively studied focusing attention towards deformation processes and microstructural changes under various test conditions at elevated temperatures [3-6]. Some studies in the area of fracture mechanism and mechanical behavior of single crystal superalloy SC16 under Low Cycle Fatigue (LCF) have also been reported in the literature to get an overview of deformation behavior and its relationship with material parameters such as volume fraction of γ precipitates, single crystal orientation, dislocation network at γ / γ′ interfaces as well as testing parameters such as temperature, strain rate, strain range etc [7-10]. The demand for development of this alloy SC16 is mainly due to its following characteristics, when compared with its polycrystalline counterpart: (a) The absence of grain boundaries and grain boundary stabilizing alloying elements leading to an increase in melting temperature higher than the solidus temperature of γ′ phase and thereby allowing a complete solution and reprecipitation of γ′ (b) An improved creep resistance in SC16 resulting in increase in operating temperature of the alloy by about 50ºC [1],[11]. In spite of numerous research investigations undertaken all over the world, the deformation behavior of single crystal alloy SC16 is still not well established. This is primarily due to the fact the deformation behavior is interrelated with several parameters such as crystal orientation, volume fraction of g precipitates, deformation induced internal stresses, strain rate, temperature, strain range etc. in a complex manner. The development of internal stresses in single crystal alloy SC16 under LCF loading and their measurement has not been reported in the literature. In this paper, a simple methodology is

described to determine internal stresses developed in the alloy SC16 under ICF loading and their dependence on temperature and strain range without altering the initial materials parameters such as crystal orientation, volume fraction and size of γ′ phase.

2. DEVELOPMENT OF INTERNAL STRESSES

Engineering materials subjected to strain controlled cyclic loading at a constant temperature and strain rate undergoes plastic deformation when the applied stress or the effective stress exceeds the internal resistance of the material. The internal resistance can be characterized as internal stresses, which may be classified as friction stress and back stress. The friction stress (σ_f) can be defined as internal stress, present in the material, which must be overcome for plastic deformation to begin. The applied stress in a given direction when exceeds a critical value, beyond which stress (σ) – strain (ε) behavior deviates from linearity and microscopic yielding occurs, the back stress (σ_b) starts accumulating in the material as a function of strain till it reaches a maximum value at the maximum strain amplitude. The friction stress is independent of straining direction. The back stress, on the other hand, changes sign during each half cycle. As it reaches a maximum value at the maximum strain amplitude, plastic deformation begins at a lower stress in the reversed direction. Professor Kuhlmann-Wilsdorf derived expressions for internal stresses from σ - ε hysteresis loop generated under low cycle fatigue loading [12]. A typical such σ - ε hysteresis loop is shown schematically in Figure 1. The yield stress (σ_y) is the critical value of the applied stress beyond which σ - ε behavior deviates from linearity and microscopic yielding occurs. The peak stress (σ_p) is the maximum stress corresponding to maximum strain amplitude. As reported in the literature Professor Kuhlmann-Wilsdorf derived expression for back stress and friction stress following a scheme based on the consideration that the hysteresis loops are reversible [12,13]. This means that the dislocation behavior, internal stress and strain distribution remain almost unchanged in successive cycles at the points of same strain and also from forward to reversed half cycle. The following fundamental equations (1) and (2), considering materials properties such σ_y σ_p and sp as obtained from σ - ε hysteresis loop (Figure 1) are used to derive expression for internal stresses:

$$\sigma_b + \sigma_y = \sigma_f \text{ ……..} (1)$$
$$\sigma_f + \sigma_b = \sigma_p \text{……} \quad (2)$$

Equation (1) holds good at the start of plastic deformation in the forward cycle i.e. at σ_y, the back stress (σ_b) generated in the preceding half cycle acts in the same direction as the stress.

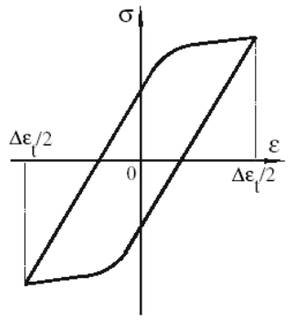

Figure 1 - A schematic σ - ε hysteresis loop under LCF loading

In contrast the back stress counteracts in the reversed direction (Equation (2)), i.e. the stress is the sum of back stress and friction stress for the plastic deformation to begin. Algebraic simplification of equations (1) and (2) leads to the expression for internal stresses σ_b and σ_f (Equations (3) and (4)).

$$\sigma_b = (\sigma_p - \sigma_y)/2 \text{ ……} (3)$$
$$\sigma_f = (\sigma_p + \sigma_y)/2 \text{ ……} (4)$$

It is thus obvious that the interrelationship of back stress and friction stress in a fully reversible hysteresis loop is yield stress dependent i.e. if (i) $\sigma_y > 0$, $\sigma_b < \sigma_f$, (ii) $\sigma_y = 0$, $\sigma_b = \sigma_f$, and (iii) $\sigma_y < 0$, $\sigma_b > \sigma_f$.

3. MATERIAL AND MICROSTUCTURE

The single crystal bars of Nickel-base superalloy SC16 with their axis parallel to [001] direction were chosen for this investigation. The chemical composition (Table-1) of the alloy SC16 is comparable with the polycrystalline alloy IN738LC used as blade material in land base gas turbines, excepting the presence of high Mo and Ta and absence of W and Co in the alloy SC16.

Table 1 - Chemical composition of the alloys SC16 and IN738LC (wt %)

Elements	Cr	Al	Ti	Mo	Ta	W	Co	C	Nb	Zr	B	Ni
Alloy SC16	16.0	3.50	3.50	3.00	3.50	-	-	-	-	-	-	Bal.
Alloy IN738LC	15.9	3.40	3.47	1.75	1.81	2.61	8.60	0.11	0.82	0.04	0.01	Bal.

The bars were subjected to the following heat-treatment cycle: (a) Solution treatment at 1250ºC for 3 hours followed by air cooling; (b) Ageing at 1100ºC for 24 hours followed by air cooling. The microstructure of the alloy SC16 in the heat-treated condition consisted of uniform dispersion of 40% γ′ precipitates coherently

embedded in γ matrix (Figure 2).The average cube edge length of γ′ precipitates was about 450 nm.

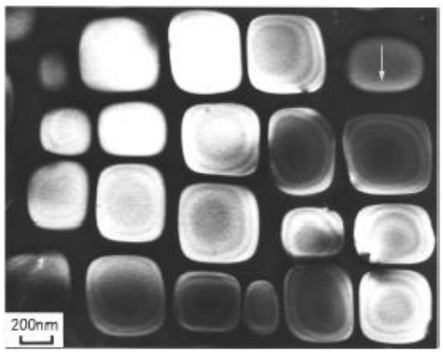

Figure 2 - Microstructure of the alloy SC16 in the heat-treated condition

4. EXPERIMENTAL

Strained controlled Low Cycle Fatigue tests were carried out using MTS servohydraulic testing machine. The fully reversed tests (strain ratio = $\varepsilon_{min}/\varepsilon_{max}$ = -1) were conducted using specimens having 9 mm gauge diameter and 12 mm gauge length, machined from heat-treated bars of the alloy SC16. The test parameters selected for LCF tests are given in Table-2.

Table 2: Test parameters for LCF Tests

Temperature ^oC	Strain Rate (/s)	Total Strain Range (%)
950	10^{-3}	0.8, 1.2, 1.6, 2.0
850	10^{-3}	0.8, 1.2, 1.6, 2.0
750	10^{-3}	0.8, 1.2, 1.6, 2.0

The methodology followed for determination of internal stresses developed under LCF loading consists of the following steps:

1. For each experiment, stress (σ) versus total strain (ε_t) hysteresis loop was generated as a function of number of cycles (N) till specimen failure and stored in a computer.

2. Stress (σ) versus plastic strain (ε_p) hysteresis loop was derived from stress (σ) versus total strain (ε_t) hysteresis loop following equation (5)

$$\varepsilon_t\,\% = \varepsilon_e(\text{elastic strain})\,\% + \varepsilon_p\,\% \ldots\ldots\ldots\ldots (5)$$

3. From each s versus ε_p hysteresis loop, the cyclic stress response of the alloy SC16 in terms of σ_y and σ_p are obtained during the forward (tensile) and reverse (compressive) loading.

4. The dependence of σ_p and σ_y on the number of cycles in the forward and reversed direction was analyzed to examine the steady state response of the alloy SC16 at constant temperature and strain range.

5. The internal stresses σ_b and σ_f and their steady state response were determined from the dependence of σ_p and σ_y on the number of cycles, using equations (3) and (4).

6. The steady state internal stress response of the alloy SC16 thus obtained under LCF loading was subsequently analyzed to examine their dependence on test parameters such as temperature and strain range.

5. RESULTS AND DISCUSSION

Figure 3(a) shows an experimentally obtained σ-ε_t hysteresis loop of the single crystal superalloy SC16 corresponding to 245th cycle under LCF loading at 950^{o}C and 1.6% total strain range.

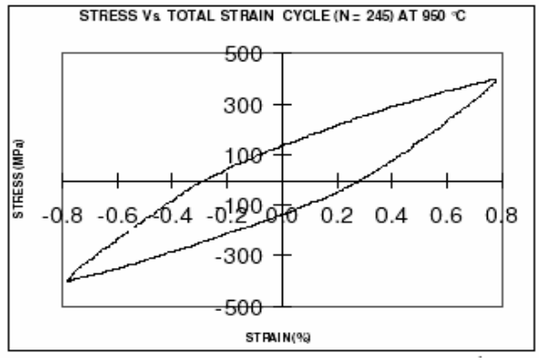

Figure 3(a) - Stress vs total strain of 245th cycle

The σ-ε_p hysteresis loop of the same cycle indicating σ_y and σ_p in the forward and reverse direction is shown in Figure 3(b).

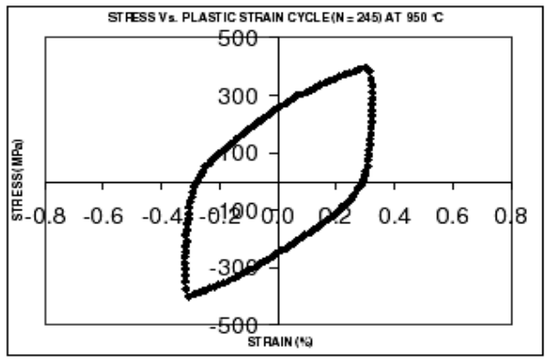

Figure 3(b) - Stress vs plastic strain of 245th cycle

The material parameters σ_p and σ_y thus obtained in the investigated range of test parameters were analyzed to examine their dependence on the number of cycles, temperature and strain range. The dependence of σ_p and σ_y on number of cycles (N) at 950°C and 0.8% total strain range are shown in Figure 4(a) and Figure 4(b) respectively. It is evident from Figure 4(a) that a steady state response of sp was almost attained after a short initial transient showing softening in first few cycles.

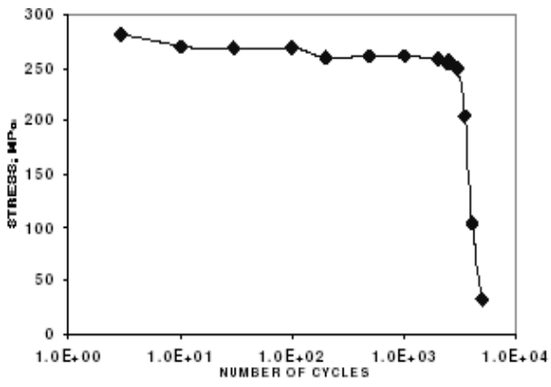

Figure 4(a) - Dependence of σ_p on number of cycles

The peak stress remains more or less stable till failure, precisely when the cyclic life consumed varies from about 4% to 50% of the number of cycles to failure (N_f). The dependence of cyclic yield stress (σ_y) on the number of cycle's exhibit similar behavior (Figure 4(b)).

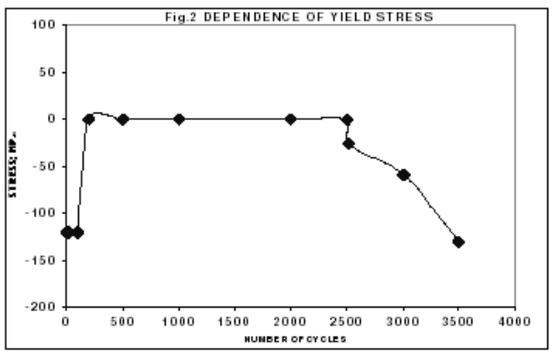

Figure 4(b) - Dependence of σ_y on number of cycles

The estimation of internal stresses i.e. σ_b and σ_f and their dependence on number of cycles (N) at 950°C and 0.8% total strain range, as obtained from the analysis of cyclic peak stress and yield stress, are shown in Figure 5(a) and Figure 5(b) respectively. A comparative evaluation clearly indicates that the internal stress response of the alloy SC16 is similar to the cyclic peak stress and yield stress response in the steady state condition, i.e. a stable steady state regime of σ_b and σ_f is attained in the useful cyclic life range of 4% to 50% of the number of cycles to failure.

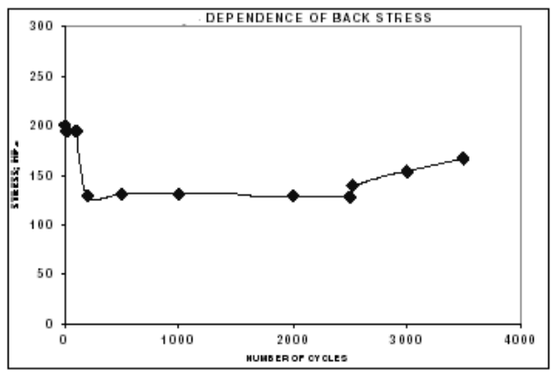

Figure 5(a) - Dependence of σ_b on number of cycle

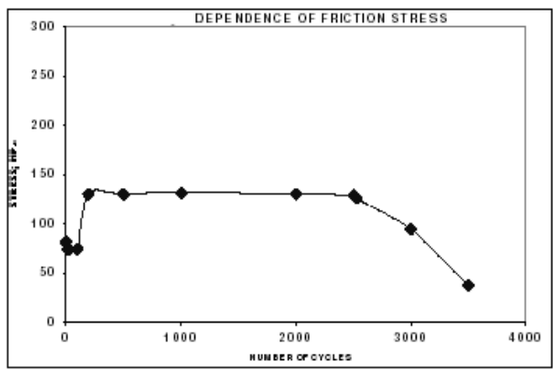

Figure 5(b) - Dependence of σ_f on number of cycle

In the reverse direction i.e. in the compressive part of the cycle, the dependence of σ_p and σ_y, as obtained from ε- σ_p hysteresis loop, on number of cycles (N) at 950°C and 0.8% total strain range are shown in Figure 6(a) and Figure 6(b) respectively. The cyclic stress response in compression was thus found to be similar to that in tension.

The steady state response of peak stress in compression indicates that after an initial softening in first few cycles, a stable steady state response is obtained in the cyclic life range of 4% to 50% of the number of cycles to failure. The cyclic peak stress response in compression was thus found to be similar to that in tension. The cyclic yield stress (σ_y) in compression also exhibit similar steady state response (Figure 6(b)).

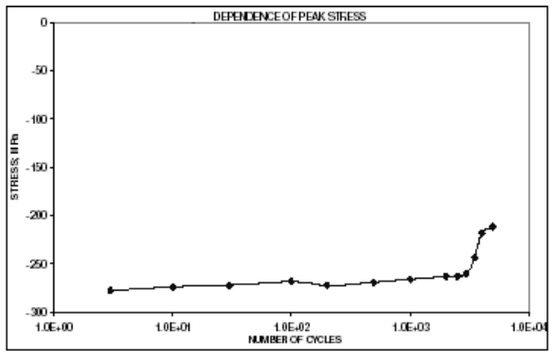

Figure 6(a)- Dependence of σ_p on number of cycle

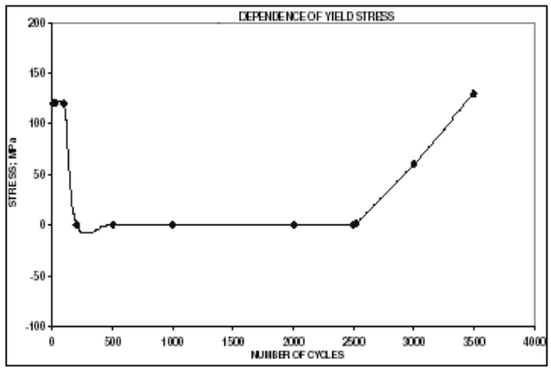

Figure 6(b) - Dependence of σ_y on number of cycle

The estimation of internal stresses i.e. σ_b and σ_f and their dependence on number of cycles (N) at 950ºC and 0.8% total strain range, as obtained from the analysis of cyclic peak stress and yield stress in compression, are shown in Figure 7(a) and Figure 7(b) respectively.

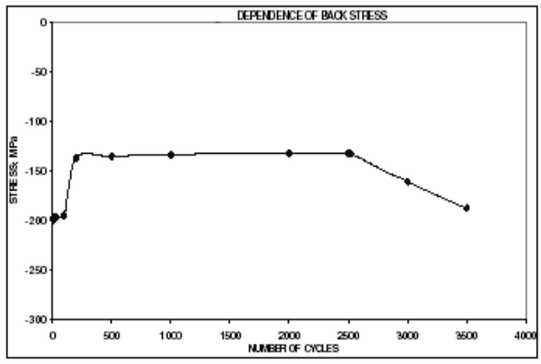

Figure 7(a) - Dependence of σ_b on number of cycle

In the compressive part of the cycle, a comparative evaluation also indicates a similar behavior as observed in the tensile part of the cycle i.e. the internal stress response of the alloy SC16 is similar to the cyclic peak stress and yield stress response in the steady state condition, and a stable steady state regime of σ_b and σ_f is attained in the useful cyclic life range of 4% to 50% of the number of cycles to failure. The nature of tensile of compressive internal stresses remains unaltered in a given direction of loading and changes its sign in the reverse direction of loading.

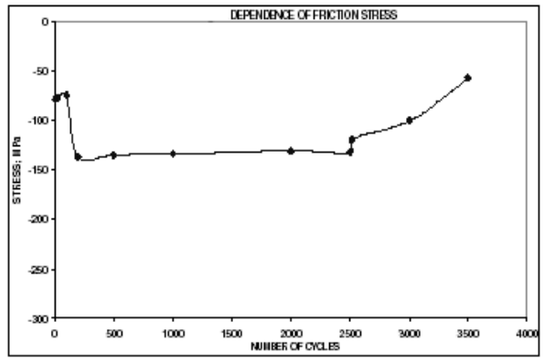

Figure 7(b)- Dependence of σ_f on number of cycle

In order to study asymmetry in cyclic stress response, the ratio of steady state tensile to compressive peak stress was estimated at 950ºC and 0.8% total strain range. The asymmetry thus obtained was found to be least pronounced since the stress ratio was close to unity.

5.1. Influence of Strain Range

The influence of total strain range on the steady state cyclic stress response and internal stresses was investigated in the temperature range of 750ºC to 950ºC. In the forward direction of loading i.e. in the tensile part of the ε - σ_p hysteresis loop, the dependence of peak stress (σ_p) and yield stress (σ_y) on total strain range ($\Delta \varepsilon_t$) at 950ºC are shown in Figure 8(a) and Figure 8(b) respectively.

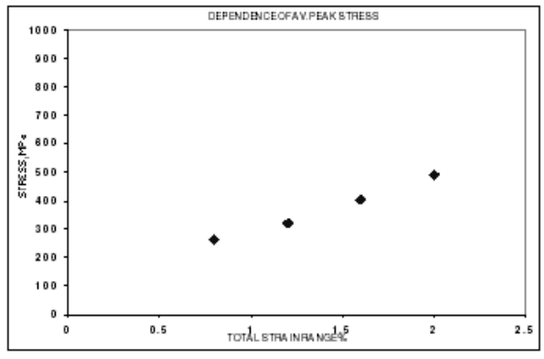

Figure 8(a) - Dependence of σ_p on $\Delta\varepsilon_t$

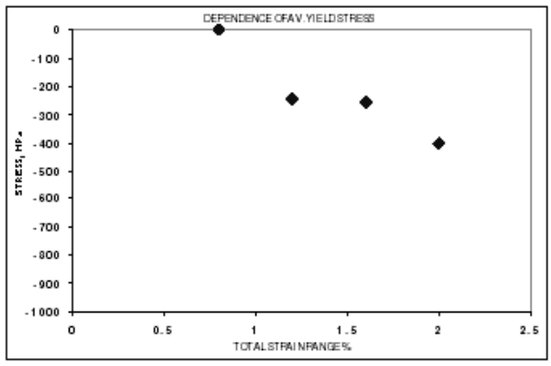

Figure 8(b) - Dependence of σ_y on $\Delta\varepsilon_t$

The steady state peak stress increases with increasing total strain range, other test parameters remaining constant. This therefore clearly indicates the dominance of work hardening behavior of the single crystal alloy SC16 with increasing total strain range. In the forward direction of loading steady state cyclic yielding occurs even before the application of tensile stress at all strain ranges at 950°C (Figure 8(b)) The compressive cyclic yield stress gradually increases with total strain range. When compressive peak stress corresponding to compressive end of total strain range is attained, the direction of straining is reversed. Thus in forward direction as evident from σ- ε_p hysteresis loop, yielding occurs at compressive stresses at 950°C irrespective of total strain range. The compressive cyclic yield stress however gradually increases with total strain range. The internal stresses (σ_b and σ_f) estimated from cyclic yield and peak stress in the forward direction using the equations (3) and (4) and their dependence on total strain range at 950°C are shown in Figure 9(a) and Figure 9(b). In forward direction both the internal stresses were found to be tensile in nature. Though the back stress increases with increasing total strain range, the friction stress does not change significantly.

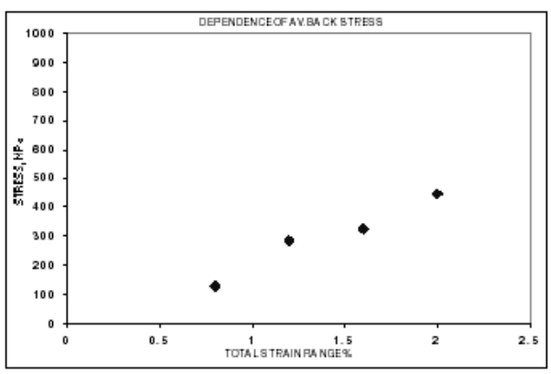

Figure 9(a) - Dependence of σ_b on $\Delta\varepsilon_t$

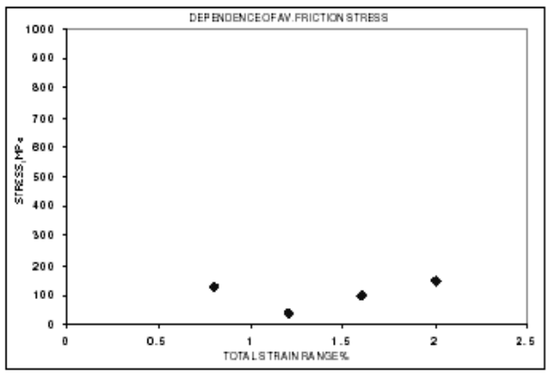

Figure 9(b)- Dependence of σ_f on $\Delta\varepsilon_t$

In the reverse direction of loading i.e. in the compressive part of the σ-ε_p hysteresis loop, the dependence of peak stress (σ_p) and yield stress (σ_y) on total strain range ($\Delta\varepsilon_t$) at 950°C are shown in Figure 10(a) and Figure 10(b) respectively. The steady state compressive peak stress increases with increasing total strain range, other test parameters remaining unaltered. The evidence of work hardening in compression was thus found to be pronounced. In the reverse direction of loading, steady state cyclic yielding occurs even before application of compressive stress at all strain ranges at 950°C (Figure 10(b)).

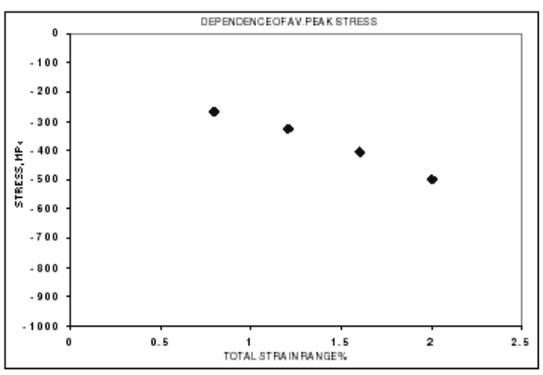

Figure 10(a)-Dependence of σ_p on $\Delta\varepsilon_t$ (In compression)

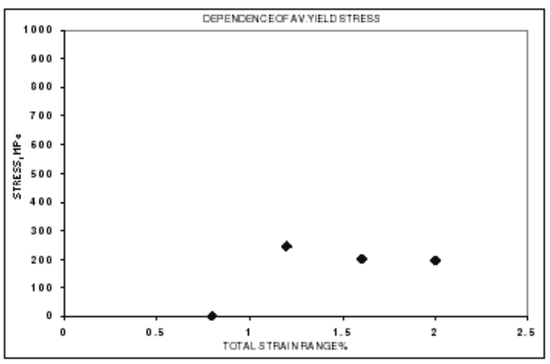

Figure 10(b)-Dependence of σ_y on $\Delta\varepsilon_t$(In compression)

When tensile peak stress corresponding to tensile end of total strain range is attained, the direction of straining is reversed. Thus in reverse direction as evident from the σ- ε_p hysteresis loop, yielding occurs at tensile stresses at 950ºC irrespective of total strain range. The internal stresses (σ_b and σ_f) estimated from cyclic yield and peak stress in the reverse direction using the equations (3) and (4) and their dependence on total strain range at 950ºC are shown in Figure 11(a) and Figure 11(b). In reverse direction both the internal stresses were found to be compressive in nature. Though the back stress increases with increasing total strain range, the friction stress does not change significantly.

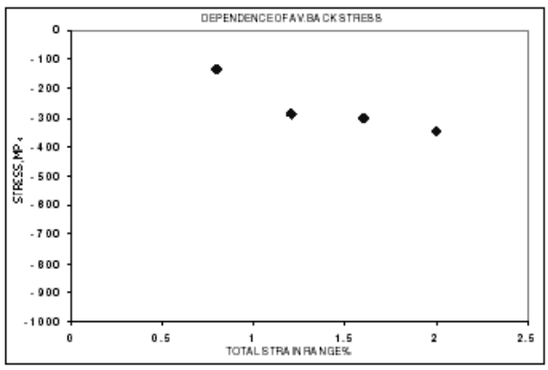

Figure 11(a)-Dependence of σ_b on $\Delta\varepsilon_t$ (In compression)

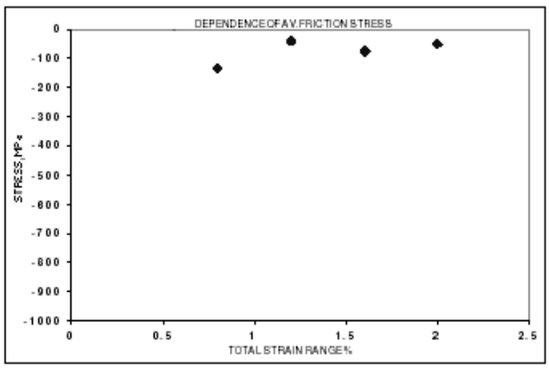

Figure 11(b)-Dependence of σ_f on $\Delta\varepsilon_t$ (In compression)

In forward direction cyclic peak stress response at 950ºC shows initial softening in first few cycles at smaller total strain range and thereafter the peak stress remains almost stable till failure. With increasing total strain range a more pronounced stable stress response is observed. The asymmetry in stress response in terms of tensile to compressive peak stress ratio is found to be least pronounced at 950ºC irrespective of total strain range since the stress ratio is close to unity.

5.2 Influence of Temperature

The influence of temperature on the steady state cyclic stress response and internal stresses was investigated in the total strain range of 0.8% to 2.0%. In the forward direction of loading i.e in the tensile part of the σ - ε_p hysteresis loop, the dependence of peak stress (σ_p) and yield stress (σ_y) on temperature (T) at 2% total strain range are shown in Figure 12(a) and Figure 12(b) respectively. The steady state peak stress decreases with increasing temperature, other test parameters remaining constant. This therefore clearly indicates the dominance of softening behavior of the single crystal alloy SC16 with increasing temperature at a given total strain range. In forward direction of loading, steady state cyclic yielding occurs even before the application of tensile stress at all temperatures (Figure 12(b)).

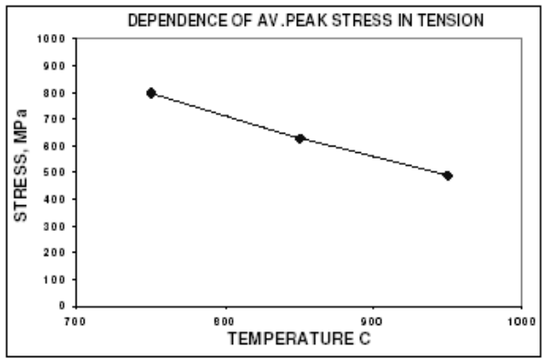

Figure 12(a)- Dependence of σ_p on Temperature

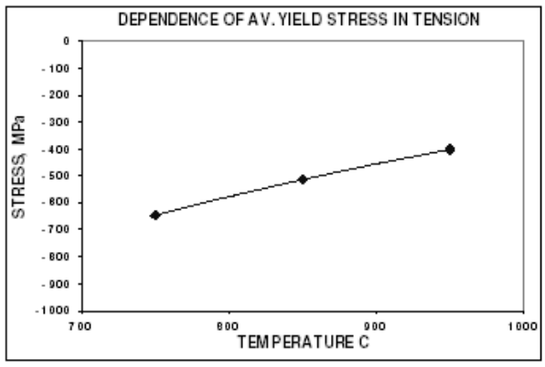

Figure 12(b) -Dependence of σ_y on Temperature

When compressive peak stress corresponding to compressive end of total strain range is attained, the direction of straining is reversed. Thus in forward direction as evident from the σ - ε_p hysteresis loop,

yielding occurs at compressive stresses at 2% total strain range irrespective of temperature.

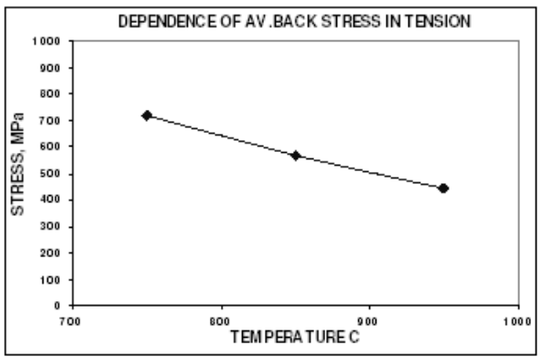

Figure 13(a) -Dependence of σ_b on Temperature

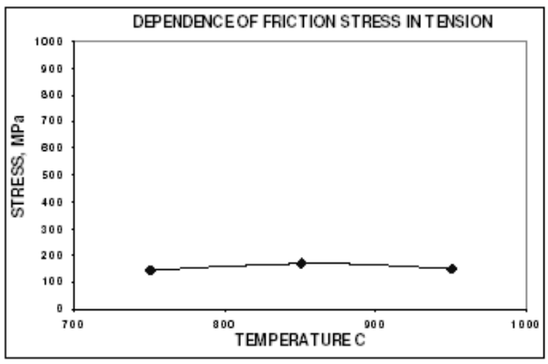

Figure 13(b)- Dependence of σ_f on Temperature

The compressive cyclic yield stress in the forward direction however gradually decreases with increasing temperature. The internal stresses (σ_b and σ_f) estimated from cyclic yield and peak stress in the forward direction using the equations (3) and (4) and their dependence on temperature at 2% total strain range at are shown in Figure 13(a) and Figure 13(b). In forward direction both the internal stresses were found to be tensile in nature. Though the back stress decreases with increasing temperature, the friction stress does not change significantly. In the reverse direction of loading i.e. in the compressive part of the σ - ε_p hysteresis loop, the dependence of peak stress (σ_p) and yield stress (σ_y) on temperature (T) at 2% total strain range are shown in Figure 14(a) and Figure 14(b) respectively. The steady state compressive peak stress decreases with increasing temperature, other test parameters remaining unaltered. The evidence of softening in compression with increasing temperature was thus found to be pronounced. In the reverse direction of loading, steady state yielding occurs even before the application of compressive stress at all temperatures at 2% total strain range (Figure 14(b)).

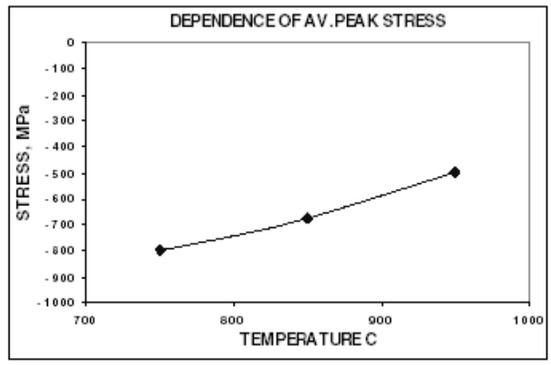

Figure 14(a)-Dependence of σ_p on Temperature (In Compression)

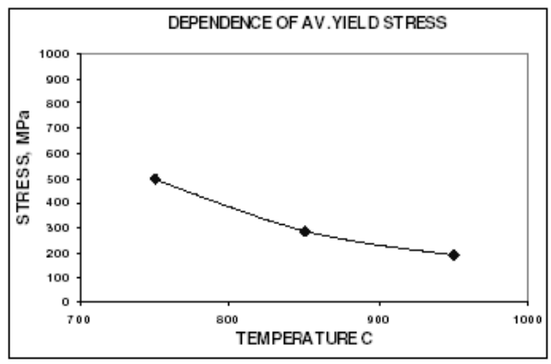

Figure 14(b)-Dependence of σ_y on Temperature (In Compression)

When the tensile peak stress corresponding to tensile end of the total strain range is attained, the direction of straining is reversed. Thus in the reverse direction as evident from the σ - ε_p hysteresis loop, yielding occurs at tensile stresses at 2% total strain range irrespective of temperature. The internal stresses (σ_b and σ_f) estimated from cyclic yield and peak stress in the reverse direction using the equations (3) and (4) and their dependence on temperature at 2% total strain range are shown in Figure 15(a) and Figure 15(b).

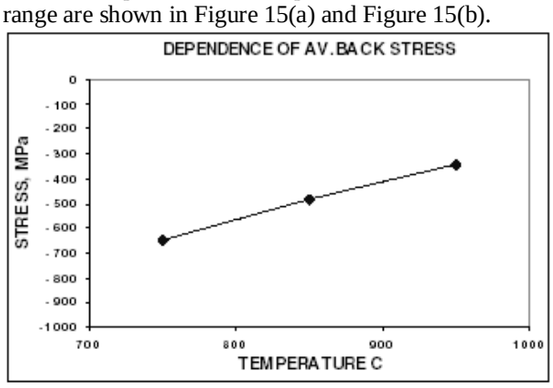

Figure 15(a)-Dependence of σ_b on Temperature (In Compression)

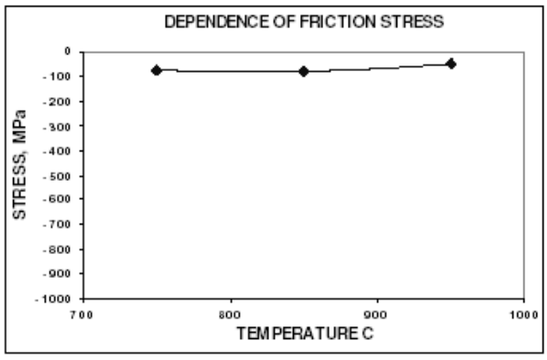

Figure 15(b) -Dependence of σ_f on Temperature (In Compression)

In reverse direction both the internal stresses were found to be compressive in nature. Though the back stress decreases with increasing temperature, the friction stress does not change significantly.

5.3 Microstructural Changes

Microstructural changes in Ni-base superalloys and their correlation with deformation behaviour have been extensively studied and reported in the literature [4] [6] [14-18]. Under monotonic loading in the high strain rate and temperature domain, stacking fault formation in γ' precipitates are observed besides formation of dislocation network at γ/γ' interface [19]. In contrast, in the low strain rate (below 10^{-7}/s) domain, microstructures consisted of mainly dislocation network at γ/γ' interface without any evidence of stacking fault formation in γ' precipitates.

6. CONCLUSIONS

The influence of temperature and strain range on low cycle fatigue behaviour of single crystal Ni base superalloy SC16 was investigated in terms of internal stresses classified as back stress and friction stress. The internal stresses are quantitatively estimated from the analysis of stress-strain hysteresis loops generated experimentally under low cycle fatigue loading. The main results in terms of dependence of back stress and friction stress on number of cycles, strain range and temperatures are as follows:

1. Both the internal stresses attain as a function of load cycles almost a steady state at a constant temperature and strain range after an initial short transition region.

Dependence on strain range at 950ºC

1. The peak stresses in both tensile and compressive direction increase with increasing total strain range.
2. The back stress is greater than the friction stress at all strain ranges except at 0.8% total strain range where they are equal.
3. The back stresses in tension as well as in compression increase with increasing total strain range. In contrast, the friction stresses are almost independent of strain range, irrespective of straining direction.

Dependence on temperature at 2% total strain range

1. The peak stresses in both tensile and compressive direction decrease linearly with increasing temperature.
2. The yield stresses in both tensile and compressive direction increase linearly with increasing temperature.
3. The back stresses in tension as well as in compression decrease linearly with increasing temperature. In contrast, there is no significant influence of temperature on friction stresses.

7. REFERENCES

1. T. Khan and P. Caron, 1990, *"In High Temperature Materials for Power Engineering Part II*, Kluwer Academic Publishers, The Netherlands, pp 1261-1270
2. J. Auerswald, D. Mukherjee, W. Chen and R.P. Wahi, Zeitschrift fur Metalkunde, 1997,vol.88,8, pp 652-658
3. R.N. Ghosh, R.V. Curtis and M. McLean, 1990, Acta Metall., 38 ,pp1977-1992
4. H. Gabrish, T. Kuttner, D. Mukherjee, W. Chen, R.P. Wahi and H. Wever, 1994, *"Microstructural Evaluation in the Superalloy SC16 under Monotonic Loading, in Materials for Advanced Power Engineering Part II*, Kluwer Academic Publishers, The Netherlands, pp 1119-1124
5. T. M. Pollock and A.S. Argon,1992, *"Creep Resistance of CMSX-3 Nickel Base Single Crystal Superalloy*, Acta Metall., vol.40, pp 1-30
6. D. Mukherjee, H. Gabrish, W. Chen, H. J. Fecht and R.P. Wahi, 1997, Acta Metall., vol.45 pp 3143-3154
7. H. J. Christ and H. Mughrabi, 1992, *"Microstructures and Fatigue, in Low Cycle Fatigue and Elasto-Plastic Behaviour of Materials"*ed. K.T. rie *et.al*, Elsevier Science Publishers Limited, London, pp 56-69.
8. T. P. Gabb and G. Welsch, 1989, Acta Metall., vol.37 pp 2507
9. D. L. anton, 1984, Acta metall., vol.32, pp 1669.
10. R. P. Wahi, J. Auerswald, D. Mukherjee, a. Dudka, H. J. Fecht and W. Chen, 1997, Internaternational

Journal of Fatigue., vol.19, Supp No. 1, pp 589-594.
11. T. Mallow, J. Zhu and R. P. Wahi, 1994, Zeitschrift fur Metallkunde, vol.85, pp.1.
12. Doris Kuhlman – Wilsdorf and Cambell Laird, 1979, Materials Science and Engineering, vol.37, pp 111-120.
13. H. Cotrell, 1953, *"In Dislocations and Plastic Flow in Crystals"*, Oxford Univ. Press, London, pp 111-132.
14. D. Mukherjee, F. Jiao, W. Chen and R.P. Wahi, 1991, Acta Metall.Mater, vol.39, pp1515.
15. W. Milligan, S. Antolovich, 1990, Metall. Transc, 22A, pp 2309.
16. B. H. Kear, A. F. Giamei, J. M. Silcock and R. K. Ham, 1986, Scripta Metall. Vol.2, pp 287.
17. M. Condat and B. Decamps, 1987, Scripta Metall. Vol. 21, pp 607.
18. H. Gabrish, Dr.-Ing. Thesis, Technical University, Berlin, Germany, 1996.
19. S. Chaudhuri, W. Chen, G. Schumacher and R.P. Wahi, *Proceedings, International Conference on Advances in Materials and Materials Processing, IIT, Kharagpur, India*, 03-05 February 2006, pp 247-262.